Available online at www.sciencedirect.com

ScienceDirect

Scripta Materialia 76 (2014) 61–64

Scripta MATERIALIA

www.elsevier.com/locate/scriptamat

Prism stacking faults observed contiguous to a {10-12} twin in a Mg–Y alloy

Dalong Zhang, Baolong Zheng, Yizhang Zhou, Subhash Mahajan and Enrique J. Lavernia*

University of California, Davis, CA 95616, USA

Received 30 November 2013; revised 23 December 2013; accepted 24 December 2013
Available online 29 December 2013

Using transmission electron microscopy, we document, for the first time, the presence of stacking faults on the (10-10) prism planes in a fine-grained Mg–Y alloy. These prism stacking faults were found to be exclusively contiguous to a {10-12} deformation twin. In addition, the {10-12} twin contained a high density of basal plane stacking faults. Arguments are developed for the interrelationship between the stacking faults on the prism planes in the matrix and those on the basal planes in the twin.

Keywords: Magnesium alloy; Transmission electron microscopy; Deformation twinning; Prism stacking faults; Partial dislocations

Despite being abundant and having low density, Mg has found limited engineering applications. As a result of its hexagonal close-packed (hcp) structure, the most common and easiest deformation mode in Mg alloys is basal slip [1], namely dislocation activity on the (0001) planes, while on the non-basal planes (e.g. {10-10} prism planes or {11-22} pyramidal planes), a high critical stress is required for slip [2]. Twinning accommodates non-basal deformation [3,4], and {10-12} twin is the most common twinning mode. The easy basal slip together with possible {10-12} twinning results in a very limited ductility during deformation [1].

Recent modeling studies suggest that alloying Mg with Y not only reduces the stacking fault energy (SFE) on the (0001) planes [5], but also reduces the cross-slip stress required for the movement of dislocations from basal to prism planes [6]. These features would theoretically result in better mechanical properties in Mg–Y alloys. Matsuda et al. [7] recently studied the interaction between {10-12} deformation twins and a long-period stacking order phase in an Mg alloy, but no attempt was made to study the interactions between stacking faults (SFs) and twins. On the basis of molecular dynamics simulations, Li and Ma [8] predicted the formation of SFs in the {10-11} plane, although, again, no experimental verification of this prediction was provided. In view of this lack of fundamental understanding on the interactions between SFs and twins, and prism dislocation activity in Mg–Y alloys, we studied an Mg–Y alloy to provide experimental insight into non-basal deformation modes, e.g. twinning and prism slip/stacking faults, and their possible interactions.

Mg–2.5 at.% Y alloy powder was synthesized by melting Mg–30 wt.% Y master alloy with pure Mg at 800 °C, followed by gas atomization in an Ar atmosphere. After hot vacuum degassing, the powder was consolidated via hot isostatic pressing and extrusion (reduction ratio 10:1) at 350 °C, resulting in a fine-grained (FG) Mg–Y alloy (grain size 1–2 μm). Cylindrical specimens, 5 mm in diameter and 7 mm in height, were machined and polished for compression along the extrusion direction (ED) at a strain rate of 10-3 s^{-1} and at room temperature. The FG Mg–Y exhibited a yield stress of ~310 MPa, an ultimate compression stress of ~430 MPa and a strain to failure of ~22%. Detailed studies of the relationship between mechanical behavior and microstructure will be reported elsewhere [9]. In this study, we specifically focus on a specimen that was deformed to ~2% strain along the ED. Thin foils for transmission electron microscopy (TEM) studies (JEOL JEM 2500 SE, 200 kV) were ground to a thickness of ~30 μm, followed by ion milling until perforation.

It is well known that, when compressed along the ED, {10-12} deformation twins form readily in Mg

* Corresponding author; e-mail: lavernia@ucdavis.edu

1359-6462/$ - see front matter
http://dx.doi.org/10.1016/j.scriptamat.2013.12.015

alloys [10,11]. Figure 1 shows part of a microsized grain in a sample compressed to ~2% strain along ED. The grain was observed in the ⟨1-21-3⟩ zone axis (Fig. 1b). There is an obvious band-like region with white contrast (Fig. 1a), indicating the presence of {10-12} deformation twins. There is also a high density of line contrast within the twin (region B in Fig. 1a), suggesting the presence of basal plane SFs [12]. In fact, basal plane SFs located inside {10-12} twins in deformed Mg or Mg alloys have been observed before [13,14]. The presence of these SFs can be attributed to the glide of partial dislocations on the basal plane [15]. The presence of Y can reduce the SFE of basal plane in Mg [5], thus enhancing the dissociation of 1/3⟨1-210⟩ dislocations into 1/3⟨1-100⟩ partials [16].

To study the twin boundaries (TBs) and SFs in more detail, dark-field (DF) images (Fig. 1d and f) were obtained using the 10-10 diffraction spot in Figure 1b. In this format, the parent grain will appear bright whereas the {10-12} twin will appear dark. Comparing the DF images (d and f in Fig. 1) with the corresponding bright-field (BF) images (c and e in Fig. 1), one can clearly see the nearly straight TBs (marked as dashed yellow lines). Interestingly, SFs not only lie in the twin, but also extend into the parent grain (e.g. SFs highlighted by yellow and red arrows in Fig. 1e) – although, for the parent grain, the (0001) basal plane cannot be viewed from the ⟨1-21-3⟩ zone axis. Instead, the orientation of the SFs in the parent grain aligns with that of (10-10) prism planes, as evidenced by the diffraction pattern in Figure 1b. Accordingly, one may conclude two observations: first, there are indeed SFs located inside the parent grain, and second these are prism SFs.

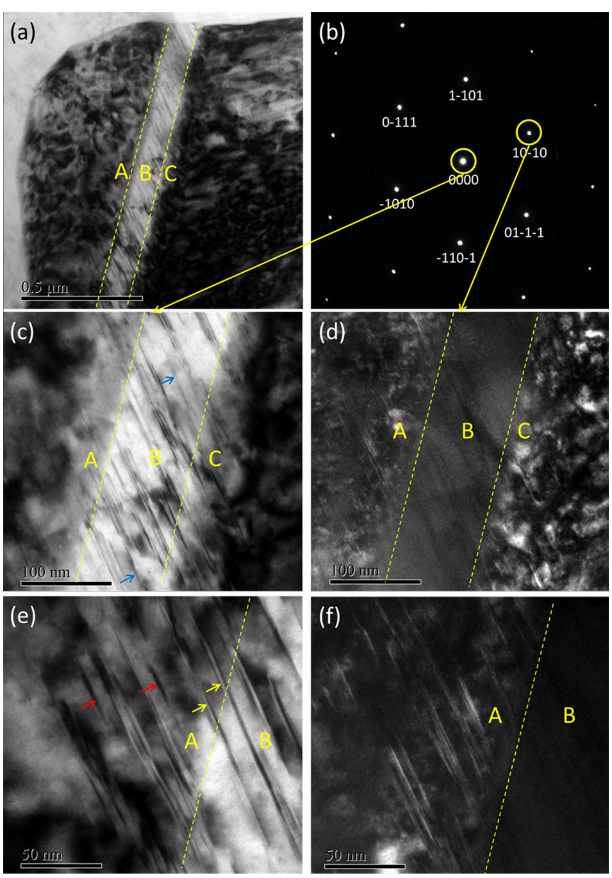

Figure 1. (a) Part of a microsized grain. (b) Selected area electron diffraction pattern of the parent grain. (c, e) Bright-field images for the {10-12} twin in (a). (d, f) Corresponding dark-field images for the same areas in (c) and (e), respectively.

It is important to note, however, that the dashed yellow lines which highlight the TBs in the BF–DF TEM analysis represent an approximate location of TBs for the following reasons. First, since the twinned region is not close to any zone axis, it is very difficult to observe the TBs precisely edge-on in TEM. Second, a twin is a three-dimensional structure, so it is possible for the twin to be inclined to the viewing plane (e.g. (1-21-3)), and thereby overlap with the parent grain in the projected TEM view. Third, real TBs can deviate significantly from the ideal {10-12} twin plane in deformed hcp materials [17], which is probably due to the steps created by twin–slip interaction. In our ongoing study on Mg–Y alloy, this deviation was also observed [9].

Therefore, to provide additional experimental evidence to the suggestion that there are SFs on the (10-10) prism planes in the parent grain, as opposed to the possibility that these are overlapping basal SFs in the {10-12} twin with the parent grain, we employed high-resolution TEM (HRTEM) and fast Fourier transformation (FFT) [18]. In reciprocal space, an SF will resemble a slender rod in appearance. Under diffraction conditions or FFT, this rod is sectioned by the Ewald sphere, resulting in a streaking that connects the diffraction spots corresponding to the planes the SF is lying in [12]. Figure 2 shows the HRTEM image of some SFs in the parent grain (e.g. region A in Fig. 1e). Figure 2b and d are FFT images for selected areas (red squared areas I and III in Fig. 2a) containing no SFs, and they are the same pattern as the diffraction pattern in Figure 1b, i.e. these areas are indeed at the ⟨1-213⟩ zone axis. For the selected area (SA) II, which contains the tip of one SF, the FFT shows streaking (highlighted by red arrows in Fig. 2c) that connects spots for the (−1010) and (10-10) planes. These observations support the suggestion that the SFs in Figure 2a are indeed prism SFs. Furthermore, Figure 2e is the inverse FFT image for SA II in Figure 2a, and it was obtained by selecting the -1010 and 10-10 pair spots; therefore it shows the (10-10) atomic planes. It is noted that there is no extra half (10-10) plane in Figure 2e, which indicates that the prism SFs are the results of Shockley partial activity in (10-10) planes, rather than the condensation of point defects [19].

At low magnification, the contrast for SFs in the twin and parent grain appears to be similar; namely, when crossing the TB, the change in contrast for two types of SFs is barely perceptible. However, when observed at high resolution at the same ⟨1-21-3⟩ zone axis for the parent grain, as evident in Figure 3a, the contrast for basal planes and basal SFs in the {10-12} twin (e.g. region B in Fig. 1e) is diffuse and unclear, unlike the contrast for prism planes and SFs in the parent grain (e.g. Fig. 2a). Figure 3b shows the FFT for a selected area in Figure 3a (red square) containing basal SFs, and the blue arrows indicate the streaking caused by basal SFs. This suggests that, in the {10-12} twin, the

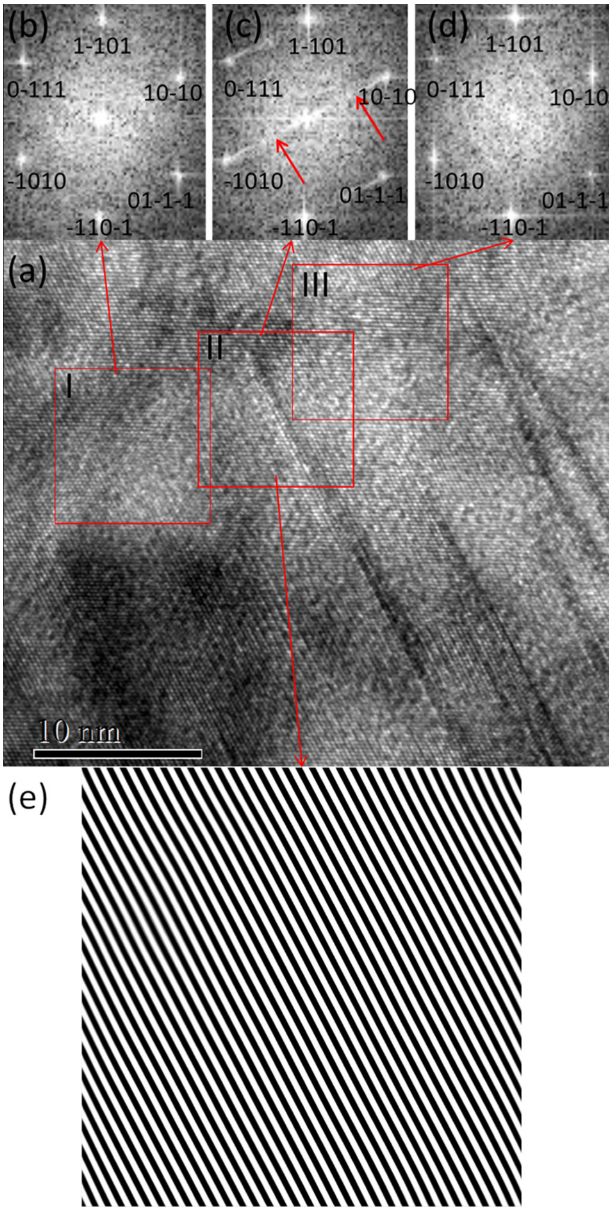

Figure 2. (a) HRTEM for prism stacking faults in the parent grain. (b–d) Selected area FFT around an SF. (e) Inverse FFT showing the {10-10} prism planes in area III.

basal planes and SFs are near edge-on, whereas other planes are not.

Experimental observations of prism SFs in other hcp materials, e.g. Ti and Zr, were first reported several decades ago [20,21]. However, this is the first direct TEM observation of prism SFs in hcp Mg alloys. It is also worth noting that prism SFs were only observed in the vicinity of the {10-12} twin (e.g. area A and C in Fig. 1c); there is no such contrast anywhere away from the {10-12} twin. Therefore, to understand the underlying mechanism(s) responsible for the formation of these prism SFs, the relationship between prism SFs in the parent grain and basal SFs in {10-12} twin was investigated, as discussed below.

Niewczas [22] calculated the mathematical transformation matrices required to link the parent lattice with

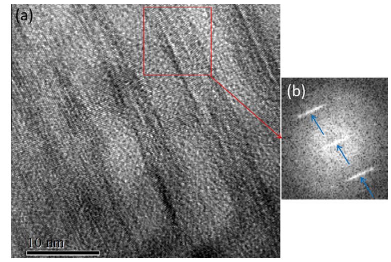

Figure 3. (a) Diffuse and unclear basal planes and SFs in a {10-12} twin. (b) FFT for a selected area in (a) (red square) containing basal SFs. (For interpretation of the references to colour in this figure legend, the reader is referred to the web version of this article.)

twinned lattice for hcp crystals. This makes it possible to quantitatively calculate the misorientation between a plane in the parent grain and a plane in a twinned lattice. For example, for a (-1 0 1 2) [10,11] twin, the misorientation between the (10-10) prism planes in the parent grain ((10-10)P) and the (0 0 0 1) basal planes in the twin ((0 0 0 1)T) was calculated to be ~2°. This calculated value is consistent with our observation that, when the prism SFs/(10-10)P in the parent grain are located edge-on at ⟨1-21-3⟩ zone axis (Fig. 2c), the contrast of basal SFs/(0 0 0 1)T in the twin can also be seen (e.g. region B in Fig. 1c). This confirms the suggestion that the twin studied here is indeed a {10-12} twin – specifically, a (-1012) [10,11] twin variant.

Niewczas [22] also summarized the possible relationship between slip systems in a {10-12} twin and that in the parent grain from a geometrical standpoint. It is noted that (10-10)[−12-10] prism slip in the parent grain can be "transformed" to (0 0 0 1) [1-210] basal slip in a (-1012) [10,11] twin [22]. It then follows that (0 0 0 1) [1-210] basal slip in a {10-12} twin could probably be transformed to (10-10)[-12-10] prism slip in the parent grain as well. Serra and Bacon [23] used computational simulations to predict the possible interaction of 1/3 ⟨1-210⟩ screw dislocation with TBs in hcp materials. They concluded that, in hcp Mg, it is possible for a 1/3⟨1-210⟩ screw dislocation in basal plane to propagate across a {10-12} TB and remain in the prism plane near the TB. In our study, careful examination of the configuration of SFs in the vicinity of the {10-12} twin reveals that there are multiple types of SFs: prism SFs (e.g. those highlighted by red arrows in Fig. 1e), basal SFs (e.g. highlighted by blue arrows in Fig. 1c) and "compound SFs" – namely, SFs with one end in the parent grain and the other end in the twin (e.g. SFs highlighted by yellow arrows in Fig. 1e). In addition, in Figure 1e there are also SFs spanning from the left part of the parent grain across the entire twin to the right part of the parent grain. These results probably suggest very dynamic partial dislocation activity across the TBs.

On the basis of the above discussion, together with the fact that there is no extra half atom plane in Figure 2e, it is proposed that the prism SFs observed here are the results of dissociated 1/3 ⟨1-210⟩ dislocations transmitted from (0 0 0 1)T to (10-10)P. Figure 4 provides schematic illustrations of the proposed partial dislocation mechanisms. First, due to the reduced basal

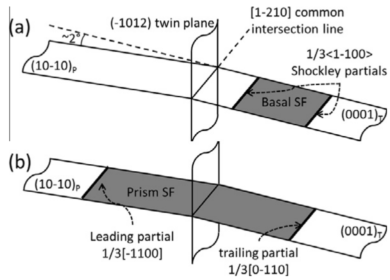

Figure 4. Schematics for formation of prism SFs.

stacking fault energy by the alloying element Y [5] and the twinning deformation [13], there are basal SFs in {10-12} twins bounded by 1/3 ⟨1-100⟩ Shockley partials [15,19,24], as shown in Figure 4a. Then, during incremental deformation, as shown in Figure 4b, some leading partials start to transmit through the TB to prism planes in the parent grain, while the trailing partials may also transmit (resulting in prism SFs) or remain in the twin (resulting in compound SFs). This transmission is geometrically possible because the three planes involved herein, namely (0 0 0 1)T, (10-10)P and the twin plane (−1012), share the same intersection line [1-210]. Therefore, for example, a 1/3[1-100] partial dislocation in (0 0 0 1)T can glide to TB, cross the [1-210] intersection line and get into (10-10)P; due to the change in indexation [22], this partial would assume a Burgers vector of 1/3[-1 1 0 0]. It is noted that whether the leading and/or trailing partials transmit through TBs or not depends largely on the local stress concentration at the TBs, so different partials would behave differently – resulting in multiple configurations of SFs, as discussed above. However, the stress required for the partial dislocations to move further into prism planes is probably much higher than that in basal planes, since it is the case for 1/3 ⟨1-210⟩ full dislocations [6]. This, we believe, is the reason why prism SFs were only observed in the vicinity of the {10-12} twin.

It is interesting to note that, mathematically, partial dislocations with a 1/3 ⟨-1 1 0 0⟩ -type Burgers vector seemingly could not glide within the (10-10)P, since none of the ⟨-1 1 0 0⟩ -type directions lie within the (10-10) plane. However, physically, the (10-10) plane is not an ideally flat plane, but rather corrugated in nature. Because of this, Rosenbaum [25] suggested that it is geometrically feasible for a 1/3 ⟨-12-10⟩ dislocation in the (10-10) plane to dissociate into two partials, namely 1/3 ⟨-1 1 0 0⟩ and 1/3⟨01-10⟩. However, in our study, further modelling work is ongoing to understand how the leading partial 1/3[-1 1 0 0] glides in (10-10)P while leaving the trailing partial behind.

In this study, SFs can be considered as "markers" that can trace the activity of partial dislocations. However, it is also possible for full 1/3 ⟨1-210⟩ basal dislocations in a {10-12} twin to transmit to prism planes in the parent grain. This suggests that twinning in Mg and Mg alloys is a very dynamic and complex process, which involves interaction between (partial) dislocations, TBs and SFs. Particularly, the possible transmission of (partial) dislocations through TBs should be examined, for it could make deformation more compatible [22]. In addition, both basal SFs and prism SFs can serve as barriers for slip in other planes [26], resulting in strengthening. For example, prism SFs can impede the easy basal slip in Mg and Mg alloys. Therefore, the Mg and hcp materials research community probably needs to take a more comprehensive approach to better understand the underlying deformation mechanisms.

Dr. T. Topping's assistance in mechanical tests is highly appreciated, as are discussions on TEM with Dr. T. Hu and Dr. L. Jiang. This work was supported by the US Army Research Office (Grant No.: W911NF-10-1-0512).

[1] M.H. Yoo, Metall. Trans. Phys. Metall. Mater. Sci. 12 (1981) 409–418.
[2] W.B. Hutchinson, M.R. Barnett, Scr. Mater. 63 (2010) 737–740.
[3] J.W. Christian, S. Mahajan, Prog. Mater. Sci. 39 (1995) 1–157.
[4] S. Vaidya, S. Mahajan, Acta Metallurgica 28 (1980) 1123–1131.
[5] S. Sandlöbes, M. Friák, S. Zaefferer, A. Dick, S. Yi, D. Letzig, Z. Pei, L.F. Zhu, J. Neugebauer, D. Raabe, Acta Mater. 60 (2012) 3011–3021.
[6] J.A. Yasi, L.G. Hector Jr., D.R. Trinkle, Acta Mater. 60 (2012) 2350–2358.
[7] M. Matsuda, S. Ii, Y. Kawamura, Y. Ikuhara, M. Nishida, Mater. Sci. Eng. A 386 (2004) 447–452.
[8] B. Li, E. Ma, Philos. Mag. 89 (2009) 1223–1235.
[9] D. Zhang, et al., in preparation.
[10] Y.N. Wang, J.C. Huang, Acta Mater. 55 (2007) 897–905.
[11] M.R. Barnett, Mater. Sci. Eng. A 464 (2007) 1–7.
[12] B. Li, P.F. Yan, M.L. Sui, E. Ma, Acta Mater. 58 (2010) 173–179.
[13] S. Morozumi, M. Kikuchi, H. Yoshinaga, Trans. JIM 17 (1976) 158–164.
[14] H.W. Pickering, P.R. Swann, Corrosion 19 (1963) 373t–389t.
[15] D.I. Tomsett, M. Bevis, Philos. Mag. 19 (1969) 533–537.
[16] J.P. Hirth, J. Lothe, Theory of Dislocations, 2nd ed., Wiley, New York, 1982.
[17] X.Y. Zhang, B. Li, X.L. Wu, Y.T. Zhu, Q. Ma, Q. Liu, P.T. Wang, M.F. Horstemeyer, Scr. Mater. 67 (2012) 862–865.
[18] D.B. Williams, C.B. Carter, Transmission Electron Microscopy: A Textbook for Materials Science, Springer, New York, 2009.
[19] J.F. Nie, Metall. Mater. Trans. A-Phys. Metall. Mater. Sci. 43A (2012) 3891–3939.
[20] K. Schwartzkopff, J. Appl. Phys. 39 (1968) 4042.
[21] P.G. Partridge, Int. Mater. Rev. 12 (1967) 169–194.
[22] M. Niewczas, Acta Mater. 58 (2010) 5848–5857.
[23] A. Serra, D.J. Bacon, Acta Metallurgica et Materialia 43 (1995) 4465–4481.
[24] S. Mahajan, D.F. Williams, Int. Metall. Rev. 18 (1973) 43–6161.
[25] H. Rosenbaum, Deformation Twinning, Gordon & Breach, New York, 1964.
[26] W. Jian, G. Cheng, W. Xu, C. Koch, Q. Wang, Y. Zhu, S. Mathaudhu, Appl. Phys. Lett. 103 (2013) 133104–133108.